Lab on a Chip

Cite this: DOI: 10.1039/c1lc20425d

www.rsc.org/loc

PAPER

Discretely tunable optofluidic compound microlenses†

Peng Fei,[a] Zi He,[a] Chunhong Zheng,[a] Tao Chen,[a] Yongfan Men[a] and Yanyi Huang*[ab]

Received 18th May 2011, Accepted 22nd June 2011
DOI: 10.1039/c1lc20425d

We report a novel method to fabricate high zoom-ratio optofluidic compound microlenses using poly (dimethylsiloxane) with multi-layer architecture. The layered structure of deformable lenses, biconvex and plano-concave, are self-aligned as a group. The refractive index contrast of each lens, which is controlled by filling the chambers with a specific medium, is the key factor for determining the device's numerical aperture. The chip has multiple independent pneumatic valves that can be digitally switched on and off, pushing the liquid into the lens chambers with great accuracy and consistency. This quickly and precisely tunes the focal length of the microlens device from centimetres to sub-millimetre. The system has great potential for applications in portable microscopic imaging, bio-sensing, and laser beam configuration.

Introduction

Optofluidics, which integrates microfluidics and micro-optical components, provides a unique solution for generating, manipulating, and controlling optical signals on a chip-based platform. Light can be guided through the liquid in micro-channels inside a chip, while microfluidic devices provide various ways to control the properties of the light propagation. Divergence control, which can be done with lenses, is important in most optical systems. Among a wealth of optofluidic devices, liquid-filled or droplet microlenses are common components, which have primarily been applied in photolithography[1] and optical imaging.[2] Recently, a new variety of on-chip assays, such as cell sorting,[3] single cell analysis,[4] and single molecule detection[5] have been widely explored to extend the applications of adaptive microlens systems. For adaptive micro-optical components,[6] especially microlenses, tunability is an essential feature. To improve the current capabilities of microlenses and to fulfil the tunability needs in many applications, dynamically tunable lenses have been intensively investigated. For light propagating in-plane, multi-convex microlenses controlled hydrodynamically using adjustable flow patterns have been reported.[7–9] For light propagating perpendicular to the chip, only a few methods have been reported to construct microlenses with adjustable focal lengths, such as liquid crystal immersed microlenses controlled by an electric field,[10] and variable focal length liquid lenses controlled *via* electrowetting.[11–14] These tunable lenses eliminate the need for optical alignment or scanning in micro-optical devices. However, liquid crystal microlenses may develop aberrations because of non-uniformities in the electric field, and the operation of electrowetting-based microlenses requires high driving voltages, which is accompanied by liquid evaporation.[15] An effective approach to making adjustable microlenses is to change the index contrast[16] by immersing the lenses in liquids with different refractive indices. Although liquid control may not be difficult, a typical drawback of replacing the liquid on-chip is the slow response speed of the device. With the wide use of poly (dimethylsiloxane) (PDMS) in microfluidic chip fabrications, a few tunable microlenses have been realized *via* injecting liquid in chambers that are made from this optically transparent elastomeric material. The shape of the microlenses can be directly tuned by adjusting the pneumatic pressure of the connected microfluidic network.[15,17,18] However, the performance of pneumatically driven lenses depends on the stability and controllability of the pressure source. This makes this type of adjustment challenging for some applications. In addition, most pneumatically tuned optofluidic microlenses are based on a single layer structure, forming a single lens with a small index contrast and narrow focal length tuning range.

A multilayer soft-lithography method[19] has been developed to fabricate complex microfluidic chips. These chips have multiple layers of crossing fluidic channels and thin deformable PDMS membranes separating them. The deformable membrane has been successfully used to construct monolithic pneumatic valves on-chip.[19,20] Here, we employ this multilayer soft-lithography technology to compound microlens devices, which consist of multiple layers of fluid chambers that serve as lens components. By digitally actuating the integrated pneumatic valves to inject tiny amounts of varied-index liquids into the chambers, the focal length of the microlenses can be changed accurately and robustly. With this simplified control mechanism using discrete actuation of integrated valves, the adjustability of the lens

[a]*College of Engineering, and Biodynamic Optical Imaging Center (BIOPIC), Peking University, Beijing, 100871, China. E-mail: yanyi@pku.edu.cn*
[b]*State Key Laboratory for Mesoscopic Physics, Peking University, Beijing, 100871, China*

† Electronic supplementary information (ESI) available. See DOI: 10.1039/c1lc20425d

performance including zoom functions can be achieved accurately and quantitatively with great fidelity. Moreover, compared with other optofluidic devices, our approach does not require apparatus to provide either stable fluidic flow or precise pressure regulation, making it more practical for many applications. This novel structure also allows for easy-to-align lens components and high zoom-ratios in microlenses.

Methods

Device fabrication

We fabricated the optofluidic chips through multi-layer soft-lithography.[19,20] The design of the chip is shown in Fig. S1a.† We printed the photo-masks on transparent films and made the mold through photolithography. The molds for the top (black, Fig. S1a†) and bottom layers (purple, Fig. S1a†) were made of positive relief patterns of SU-8 photoresist (Fig. S1c.1, S1c.3†) on silicon wafers. The mold for the middle fluidic layer (green, Fig. S1a†) was a hybrid pattern made of AZ®P4620 (AZ Electronic Materials, Branchburg, NJ, USA) photoresist (the channel part) and SU-8 (MicroChem, Newton, MA,USA) photoresist (the chamber part) (Fig. S1c.2†).

After a 24 h reflow, the channels became rounded and smooth. This treatment ensured the replicated PDMS channel was fully closed by control valves in the subsequent chip operations. Then we peeled the cured PDMS replicas off the mold, punched the inlet holes (Fig. S1c.1†), placed them on the freshly cured middle fluidic PDMS layer (thickness $\approx$ 150 μm). Then we aligned the patterns and bonded the two layers through baking (Fig. S1c.2†). Next we repeated the steps to align and bond the middle layer with the bottom layer, which serves as the control layer (thickness $\approx$ 200 μm) with valves (Fig. S1c.3†). With another repetition of the bonding step to seal the channels inside the bottom layer with a flat PDMS film, we combined these PDMS slabs into a monolithic piece with three layers of aligned micro-channels and chambers (Fig. S1c.4†). The holes, punched during the chip fabrication, were connected to compressed air *via* tubing for liquid injection and valve actuation. Fig. S1c.5† shows a completely fabricated device.

Imaging setup

We drew arrays of the micro-letter "F" (50 μm × 30 μm) using AutoCAD (Autodesk, San Rafael, CA, USA) and printed them onto a transparent film. Then we attached the film on the back of the chip. An upright microscope and a monochrome CCD camera (QHY CCD, IMG 2*S*) were used to collect the images through the microlens chip. Meanwhile, another stereomicroscope and another CCD camera (QHY CCD, IMG 2*S*) were aligned to monitor the deformation process from the side of microlens chip (Fig. S1b†).

Numerical simulations

A 3D-model was built according to the boundary conditions and parameters of a real microlens device (Fig. S2a†). It simulated the architecture of the microlens chip.[15] (Fig. S2b†). Through symmetry, the model could be split in half, which is shown in Fig. S2c.† The PDMS membrane was designed to tolerate a hydraulic pressure of $P = 0.1$ MPa. The tensile modulus, E, and Poisson ratio, u, of PDMS were also defined (E = 1.8 MPa,[21] $u = 0.4$). We obtained the displacement distributions inside the PDMS membrane and picked 10 isotonic displacement states from 0–100 μm based on the displacement of the central point A (Fig. S2d†). Then, we calculated the small difference between the inner and outer curvature radii in each state. The results were used to amend the optical simulation.

We used the Zemax EE (Bellevue, WA, USA) software package to simulate the light propagation through compound microlenses and estimate the focal lengths for different shapes. We specified the indices of the media between every two adjacent surfaces. In our experiment, they are air, fluorocarbon oil and PDMS. We defined the deformation states by dividing the vertical displacement of central point "A" on membrane's outer surface into 20 steps with a 5 μm grid size. Then, we calculated the focal length of the compound microlens for every state.

Results and discussion

Operational principle

The compound microlens chip, which is shown in Fig. 1, is completely fabricated from PDMS through a multilayer soft lithography process. The chip consists of three vertically aligned functional layers. Each layer in the chip has a round chamber connected to a channel *via* an inlet for liquid injection. Fig. 1b shows a detailed schematic of the chip. The middle chamber is 700 μm in diameter, and is sandwiched between two chambers with slightly larger diameters (1 mm) on top and bottom. In the middle layer, a few rectangular chambers, which intersect with the channel connected to the round chamber and their overlapping chambers in the bottom layer, act as the integrated pneumatic valves (Fig. 1c). We apply pneumatic pressure to the bottom layer to actuate the valves. There is a thin elastic membrane of PDMS between each of the two adjacent layers of the chambers. As the key functional element of the device, these membranes deform under uneven pressure among chambers.

Similar to the valves, the three round chambers are separated by two thin PDMS membranes, which when deforming can form a middle liquid-filled chamber with two curvature-adjustable surfaces. Thus we get a tunable microlens with an adjustable focal length *via* pressure-difference control. However, it is still challenging to accurately and promptly adjust the pressure to control the shape of the microlens. To overcome this challenge, we controlled the volume of liquid injected into the middle chamber, instead of trying to control the pressure-difference directly. This is made possible by the fully explored intrinsic properties of PDMS. At suitable pressure, dead-end channels can be completely filled with liquid, because PDMS is gas permeable. We create a closed section of liquid by closing the last valve along the channel, which is connected to the round micro-chamber in the middle layer. The volume of the injected liquid is determined by the volume of the round chamber and the rectangular chambers.

When the pneumatic valves are sequentially closed, the liquid can be extruded into the round chamber to inflate the PDMS membranes and form a biconvex microlens. This lens can undergo discrete focal length changes *via* volume adjustment.

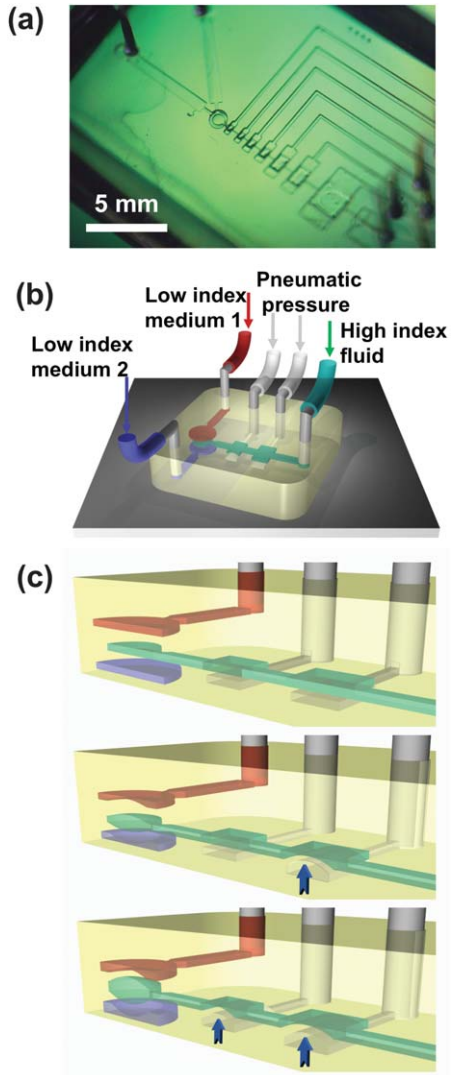

Fig. 1 A three-layer compound microlens chip with operational principle. (a) A microphotograph of a three-layer microlens chip fabricated using soft lithography. (b) In each layer and each individual channel of the chip, the chambers can be filled with arbitrary fluids to achieve different index contrast. The inlets of the integrated pneumatic valves are connected to an external solenoid pump system through micro-bore tubing for actuation. (c) As the pneumatic valves on the bottom layer are sequentially closed (indicated by arrows), fluid inside the channel in the middle (green) is discretely extruded into the round chamber to inflate the PDMS membranes and actuate three-layer shape-tunable microlenses.

Along with the expansion of the middle chamber from planar to biconvex shape, the top and bottom chambers simultaneously become concave shapes, which act as plano-concave lenses. A dynamically tunable compound microlens, with one biconvex lens and two plano-concave lenses, is completed. One of the unique features of the device is that the adjacent lenses share the same deformable PDMS membrane, ensuring that the axes of those lens dynamically formed on both sides of the membrane are automatically aligned to the middle one, even when the chambers themselves are not perfectly aligned. This feature makes "self-aligned" compound microlenses possible. Indeed, the alignment of layers is done manually under stereo microscope with limited accuracy. Typically the accuracy of the alignment between PDMS layers can reach ~10 micrometres. Both the upper and lower chambers are larger than the middle one, allowing a >50 micrometre tolerance of off-alignment. Without the "self-aligned" feature it would be impossible to fabricate compound microlenses with good imaging performance.

The actuating process is shown in Fig. 1c. When these two plano-concave chambers are empty, because the refractive index of air inside the chambers is much smaller than that of the surrounding PDMS ($n_{air} = 1$, $n_{PDMS} = 1.47$), they will act as normal positive lenses, and incident light will converge. However, if they are filled with a liquid with a refractive index larger than that of the PDMS, they will act as negative lenses, and incident light will diverge. In comparison with single layer microlens devices,[15] our compound microlens chip has more deformable components. Furthermore, the introduction of negative plano-concave air lenses ensures a large index contrast. Thanks to these two aspects, the compound lens has a much larger tunable range of focal length, which implies that a bigger magnification can be obtained. This is definitely desirable in many applications in imaging and light beam configurations.

3-layer *vs.* 2-layer architecture

Although the fabrication process gets more challenging when the device gets more layers, a chip with more lens components will converge light better. To compare the tuning range of a 3-layer microlens with that of a simpler 2-layer one (Fig. 2a and Fig. 2b), we applied the finite element method to calculate the deformation degree of the PDMS membrane, which is caused by the

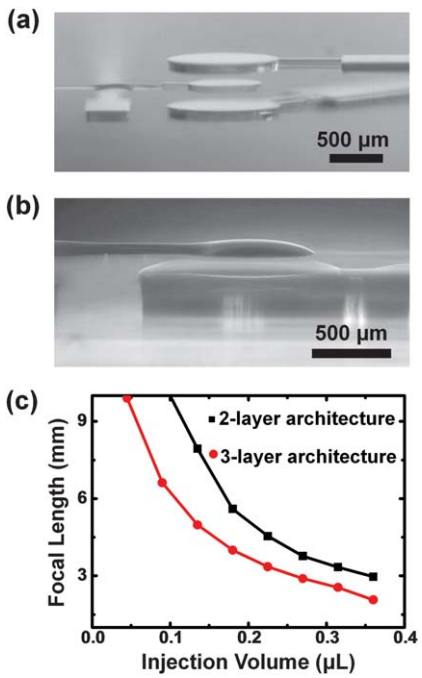

Fig. 2 (a) Microphotography of a 3-layer compound microlens. The middle liquid lens is sandwiched between two air lenses. (b) A 2-layer compound microlens with a fluid lens on top and an air lens below. (c) The simulated variations in the focal length for both 2-layer and 3-layer structures of the same diameter.

volume change through the valve actuation, and to simulate the optical propagation. With the simulated lens shapes, the light propagation pathways through the lenses were tracked and the focal lengths of the lenses for different shapes were estimated. In Fig. 2c, we plotted the variation of the focal length for both 3-layer and 2-layer compound microlenses. A 3-layer structure has an advantage over a 2-layer one because it offers a wider tuning range of its focal length. Therefore, with the same amount of liquid injected into the middle chamber, it is able to reach shorter focal lengths, which means it has a larger numeric aperture and a stronger ability to converge a light beam.

Discrete tunability

The deformable membranes of the control valves can swiftly press the corresponding rectangular parts of the fluidic channels located above them. A proper working medium should satisfy a few pre-set criteria: (1) It does not penetrate or evaporate through PDMS, even under the positive pressure. (2) It does not swell the PDMS. (3) To eliminate the reflectance between interfaces, the difference between the refractive indices of the liquid and PDMS cannot be too large. (4) For easy injection and fast response during the valve actuation, the viscosity cannot be high. In the experiment, we filled the fluidic channel in the middle layer with fluorocarbon oil (Reliber PF-6802). This fluorocarbon oil has a relatively low viscosity and great optical transparence through a large span of the optical spectrum. Another factor is that the lensing capacity of our design is greatly enhanced by the two negative air lenses, therefore fluorocarbon oil, with a relative low refractive index ($n = 1.39$, similar to PDMS), has only very limited effect. After the liquid had replaced all the air inside the micro-channels, we closed valve 1 (Fig. 3a) to cut off the fluidic channel at the other end and created a separate section of liquid.

Then we closed valves 2–7 sequentially by applying a pressure of 0.15 MPa. Actuated discretely, the valves drove the fluid along the channel into the microlens chamber. During the operation, we captured images of every state of the valves and the liquid microlens (diameter 700 μm, Fig. 3a). Fig. 3b shows the deformation details of the microlens. When the valves were closed sequentially, the liquid microlens accumulated more and more fluorocarbon oil, which further deformed the PDMS membranes on both sides. The empty air lenses above and beneath it were simultaneously squeezed. The responsive time depends on the volume changed by valve actuation. In our current devices, the responsive time is about 100 ms. The imaging change triggered by valve actuation becomes stable within 1 s. During the membrane inflation, the radius of curvature of every lens increased discretely in accord with the actuating of the control valves. Correspondingly, the focal length of the whole compound lens was reduced discretely. To evaluate the imaging properties of the microlens chip, we placed the chip on a transparent film with an array of the letter "F" (50 μm × 30 μm), which serves as an object for observation (Fig. 3d). The objective distance was fixed and determined by the thickness of the bottom layer of the PDMS. We sequentially closed the control valves and took images at all actuation states (Fig. 3c).

In the initial state, none of the valves were actuated and the microlens chip could not converge incident light, which indicates the chip was a flat optical window and had an infinite focal length. As the valves were actuated one by one, the middle convex lens became thicker and thicker, and the virtual image of the letter "F" became larger and larger. When we closed the last

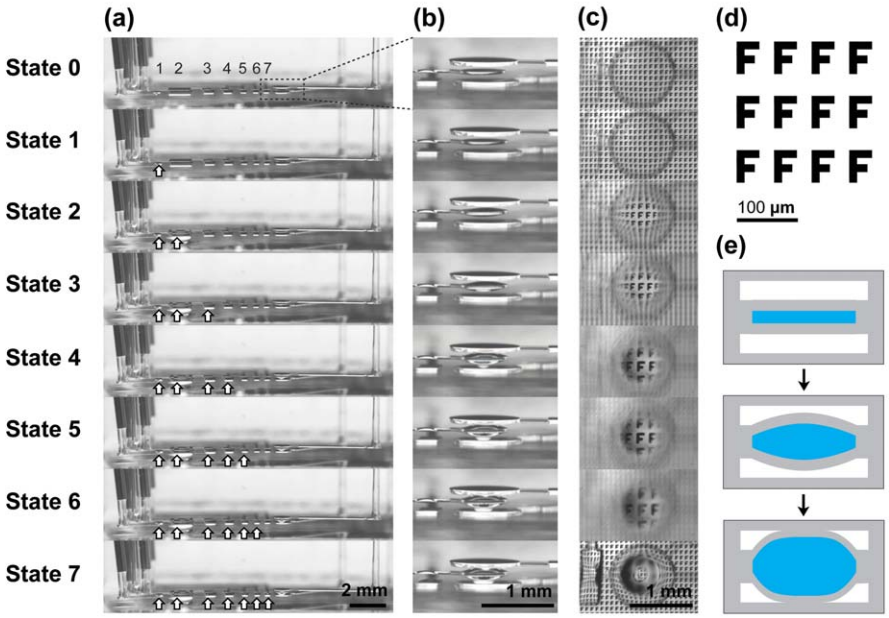

Fig. 3 (a) From state 1 to state 7, seven pneumatic valves were closed sequentially from left to right. The actuated valves (indicated by arrows) discretely extruded liquid into the microlens. (b) The deformation of the components of the microlens. Images are taken through a side-view microscope. (c) Images taken through the compound microlens. The distortion of the image after the last valve's actuation were observed. (d) The array of the letter "F" as the object. (e) When too much liquid is squeezed into the middle chamber, the deformed PDMS membrane will eventually touch the bottom of the empty chambers on both sides. This is the limit of the tunability of microlenses, as we observed in state 7.

valve, which was nearest to the microlens, the curved PDMS membrane touched the bottom of the air chambers. This is when the compound microlens reaches its limit (Fig. 3b.7, 3c.7). The image magnification at every state was calculated through the images in Fig. 3c. By combining the resulting magnification with fixed objective distance, we measured the tuning range of the focal length to be 7 to 1.2 mm in a four-level microlens chip, and to be 3.2 to 1.4 mm in a different six-level chip with finer tuning steps. Furthermore, the tuning range and step number can be designed to cover different spans, from less than 1 millimetre to over a few centimetres, with increased precision of the control steps.

To make the "zoom microlens" concept intuitively clear, we performed another experiment to test the light focusing ability by taking transmitted images *via* a CMOS sensor chip (Gsou, Model T10, China; sensor size 3.2 × 2.4 mm with pixel pitch size 5.5 μm) placed behind the lenses. While actuating the valves, we took the images of a collimated laser beam (473 nm), which propagated through a microlens with an aperture diameter of ~500 μm. First, we fixed the distance (1 mm) between the microlens chip and the CMOS sensor. When more liquid was squeezed into the middle layer of compound microlens, the focal length of the lens was reduced, the convergence angle of the transmitted beam was increased, hence the size of the laser speckle on the sensor was reduced.

This continued until the beam was focused to a small clear spot after we actuated the valves (Fig. S5.0–Fig. S5.5,† with actuation of different numbers of valves). According to Rayleigh's criterion, light transmitted through a microlens will be focused into an Airy speckle at the corresponding focal plane with a radius proportional to the *f*-number (*f*/*D*, where *f* and *D* are the focal length and aperture diameter of the microlens, respectively).[22] Through these captured images, we estimated this 500 μm compound microlens had a maximum numerical aperture (NA) of ~0.3.

Extra tunability and optical simulations

The two empty chambers not only offer free space to allow the expansion of the middle chamber in compound microlenses, they also provide an extra degree of tunability, because they can as well be filled with liquids of different refractive indices. We picked a working state for our chip, and then injected fluorocarbon oil into the air lenses on both sides, while keeping the other parameters constant. Fig. 4a shows that right after the liquid was injected into the plano-concave chambers, the image changed instantly through the drastic reduction of magnification. In our construction, the structure of the curved microlenses is derived from the deformed PDMS membranes, whose maximum curvature is determined by the heights of two symmetrical chambers on both sides. By controlling the thickness of the photoresist molds and properly setting the aperture size of the liquid microlens, we may precisely determine the tuning span of the microlens. To optimize the structural design of the chip, we performed simulations of the optical light path for each design with different parameters for each component in the compound microlens. The result of simulation was essential in guiding our fabrication of a high-quality compound microlens. In most experiments, we fabricated a compound microlens with aperture diameter of 700 μm. The height of the two air chambers was set to be 100 μm, which limited the maximum vertical displacement that the PDMS membranes could reach. In our simulation, we defined the deformation states by dividing the vertical displacement of central point "A" on membrane's outer surface into 20 steps with a 5 μm grid size, and we calculated the focal lengths of the compound microlens in each case, as plotted in Fig. 4b. With the expansion of the middle chamber filled with fluorocarbon oil, the focal length of the whole compound lens decreased to its minimum near 1 mm.

Since the membranes have boundaries that connected to the bulk part of the PDMS chip, there will be strain inhomogeneity existing in the deformed membranes when subjected to a hydraulic pressure. The radius of curvature of the deformed PDMS membrane's inner surface should be different from that of the outer surface, generating a difference between the curvature of the liquid microlens and that of the air microlenses. To estimate the optical effects caused by the strain non-uniformity, we used the finite element method to analyze the mechanical deformation of the PDMS membranes. With the amended data, also shown in Fig. 4b, from this mechanical simulation, we did the optical simulation again and compared new results with the original ones. The comparison showed insignificant differences with deviations ranging from 4.9% to 9.1%, which indicated that the simplification of the deformation for the optical simulation was sufficient to guide our design. Furthermore, from experimental results, we could calculate the corresponding focal lengths of the microlens chip using the fixed distance and varied magnifications (Fig. 4c). The maximun magnification power of this chip is 8. The focal length and corresponding numerical aperture results from the experimental data were plotted together with those from the simulation, and they agreed well with each other (Fig. 4d). From the result we estimate the optical zoom ratio of this compound microlens is about 7. Although the resolving power of the chip-based microscope can be further improved by stacking more lenses together, it would be challenging to exceed 3 layers in a single chip. One solution to this dilemma is to stack multiple chips together.

Performance of microlenses

We performed a number of tests to explore the microlens chip's feasibility in imaging applications. The epithelial cells of *Tradescantia albiflora* were employed for microscopic observation, and the results are shown in Fig. 5a. Through a microscope, with the help of a compound microlens to form virtual images, we achieved a larger magnification. The microlens chip could also form real images when properly configured. We used the microletter "F" (50 μm × 30 μm) as the object with an objective distance of 2 mm. Through the expansion of the microlens, we observed that the image formed through the chip changed from magnified virtual images to magnified real images, then eventually to a reduced image (Fig. 5b). The magnification ratio of the real image in this configuration was about three. This ratio can be increased through improvement in chip design and measurement setup. The microlens can also work independently as objective lens for microscopic observation. We integrated a high power light emitting diode illuminator and a small webcam CMOS sensor (Gsou, Model No. T10, China) for image acquisition. The

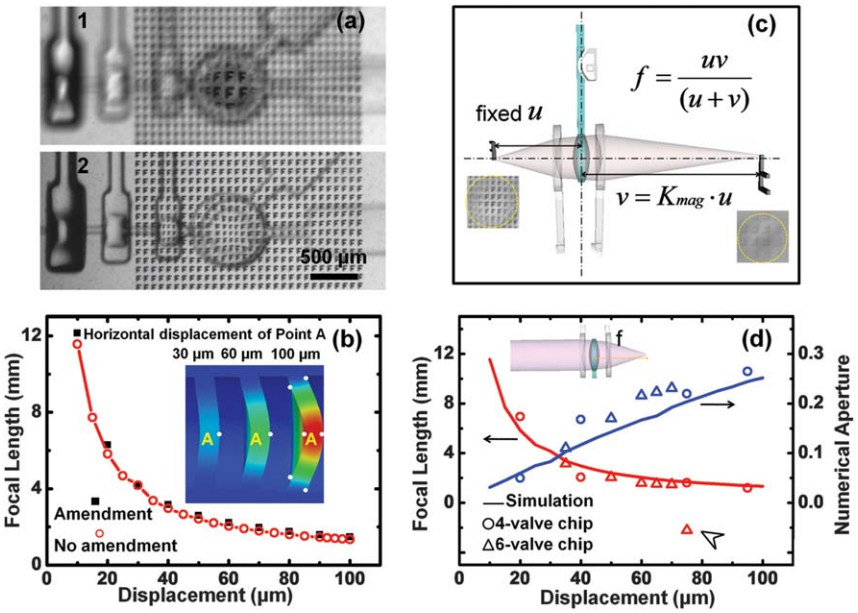

Fig. 4 (a) An actuated compound microlens with empty top and bottom lenses. In picture 1, a magnified image of the letter "F" is shown. In picture 2, the size of the letter "F" reduced drastically when the top and bottom lenses were filled with fluorocarbon oil. (b) The simulation results of the focal length of the microlens, with and without taking strain inhomogeneity of the PDMS membrane into account. The inset picture is an illustration of how the deformation process is defined by a horizontal displacement. (c) The calculation of the focal length of a tunable microlens chip during experimental processing. (d) The simulated and experimental results of the focal length (red plots, left axis) and numerical aperture (blue plots, right axis), which demonstrates the tunability of the compound microlens. The bad data point marked by the open arrow shows the deformation limit of the microlens during actuation, determined by the geometry of the device. When we inject too much liquid into the middle chamber, the PDMS membranes would finally touch the bottom of the air chambers, and the central region of the microlenses malfunctions: it fails to properly magnify and causes the aberration of images (see Fig. 3b.7, 3c.7, and 3e).

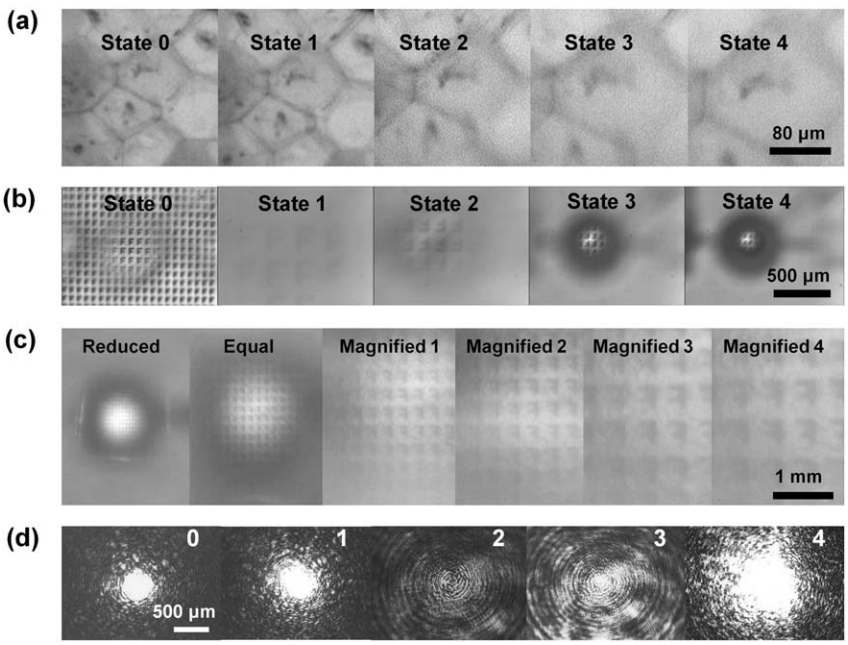

Fig. 5 Applications of a compound microlens chip. (a) Magnified virtual images of *Tradescantia albiflora* epithelial cells. Images were obtained using a 5× microscopic objective cascaded with a 4-level discretely tunable microlens chip. (b) Images of the letter "F" (50 μm × 30 μm). The change from a magnified virtual image to a magnified real image, and eventually to a reduced image was observed during the sequential actuation of the valves. (c) Images of the letter "F" (50 μm × 30 μm) were captured using microlens as an independent microscopic objective. (d) The laser beam profiles captured through two tunable microlenses operating as a beam expander. 0. The original incident beam speckle. 1. The beam speckle through the beam expander without actuation. 2. The beam speckle when only the input microlens was actuated. 3. The beam speckle when only the output microlens was actuated. 4. The expanded beam speckle when both microlenses were actuated to desirable focal lengths.

tunable viewing angle of the microlens varied from 80 to 15 degrees. Fig. 5c shows the images obtained from this miniature "microscope".

In addition to the imaging applications, we aligned two compound microlenses to serve as a miniaturized beam expander–reducer. We propagated a laser beam (~500 μm in diameter) through their center, and captured transmitted laser patterns of different sizes on a webcam CMOS sensor by tuning the focal length of each microlens chip (Fig. 5d).

Optofluidic microlenses can be easily designed to pack together as an array and this would be useful to observe multiple specimens simultaneously with flexible tunability. We have demonstrated a small array with four lenses and each of them can be controlled individually (Fig. S4†). The density can be further improved but it would be limited by the necessary space taken by microfluidic channels and valves.

Conclusions

In summary, we report a novel method of building optofluidic microlenses with excellent flexibility, robustness, and simplicity. This method meets the challenges that optofluidic microlens-builders have been facing for over a decade, and we believe, can be adapted to many applications in the field of optics. We successfully constructed a compound microlens system with multiple lens elements self-aligned together inside a monolithic micro-chip with PDMS, a gas permeable elastic polymer. The gas permeability of PDMS allows dead-ended micro-channels and micro-chambers to be completely filled with liquid, and the elasticity of PDMS ensures the deformation of thin membranes for tuning the lens. We also developed a simple, precise and robust tuning mechanism. By discretely actuating pneumatic valves integrated on-chip, we can adjust the shapes of lenses precisely, providing multiple possibilities for potential applications. Compared with other reported approaches, this method is an excellent demonstration of the power of compound microlenses, with superior optical performance such as easier self-alignment, higher zoom ratio (7–8×), wider tuning angle of view (15–80 degrees), larger range for focal adjustment (from mm to cm), bigger numeric aperture (up to 0.44) and smaller lens-size (a few hundred micrometres in diameter). A few important applications, such as the imaging and adjustment of laser beam size, are also covered in this paper. We anticipate this microlens system has the potential to provide an inexpensive and compact solution to imaging and microscopic observation, which is traditionally performed by bulky equipment. These microlens components can also be integrated with each other or with a wide range of microfluidic devices for a variety of optical and biosensing applications.

Acknowledgements

The authors thank Zitian Chen, Wentao Li and Jie Shen for their fruitful discussion. Funding for this work was kindly provided by the National Natural Science Foundation of China (20705003, 20733001, 20890020), Beijing Natural Science Foundation (2082011), the Ministry of Science and Technology of China (2007CB714502, 2009AA04Z309), the Ministry of Education of China (FANEDO200730, RFDP20070001063), and the State Key Laboratory for Mesoscopic Physics.

Notes and references

1 M. H. Wu and G. M. Whitesides, *Adv. Mater.*, 2002, **14**, 1502.
2 B. Javidi, O. Matoba and E. Tajahuerce, Optomechatronic Systems II, H. S. Cho, Ed., Proc. SPIE, 2001, **4564**, pp. 1–12.
3 M. M. Wang, E. Tu, D. E. Raymond, J. M. Yang, H. C. Zhang, N. Hagen, B. Dees, E. M. Mercer, A. H. Forster, I. Kariv, P. J. Marchand and W. F. Butler, *Nat. Biotechnol.*, 2005, **23**, 83–87.
4 B. Huang, H. K. Wu, D. Bhaya, A. Grossman, S. Granier, B. K. Kobilka and R. N. Zare, *Science*, 2007, **315**, 81–84.
5 T. H. Wang, Y. H. Peng, C. Y. Zhang, P. K. Wong and C. M. Ho, *J. Am. Chem. Soc.*, 2005, **127**, 5354–5359.
6 U. Levy and R. Shamai, *Microfluid. Nanofluid.*, 2008, **4**, 97–105.
7 X. L. Mao, J. R. Waldeisen, B. K. Juluri and T. J. Huang, *Lab Chip*, 2007, **7**, 1303–1308.
8 M. Rosenauer and M. J. Vellekoop, *Lab Chip*, 2009, **9**, 1040–1042.
9 S. K. Y. Tang, C. A. Stan and G. M. Whitesides, *Lab Chip*, 2008, **8**, 395–401.
10 L. G. Commander, S. E. Day and D. R. Selviah, *Opt. Commun.*, 2000, **177**, 157–170.
11 T. Krupenkin, S. Yang and P. Mach, *Appl. Phys. Lett.*, 2003, **82**, 316–318.
12 S. Kwon and L. P. Lee, *Transducers '01: Eurosensors Xv, Digest of Technical Papers*, 2001, **Vols. 1 and 2**, 1348–1351.
13 H. Huang, X. L. Mao, S. C. S. Lin, B. Kiraly, Y. P. Huang and T. J. Huang, *Lab Chip*, 2010, **10**, 2387–2393.
14 Y. Gambin, O. Legrand and S. R. Quake, *Appl. Phys. Lett.*, 2006, **88**, 174102.
15 N. Chronis, G. L. Liu, K. H. Jeong and L. P. Lee, *Opt. Express*, 2003, **11**, 2370–2378.
16 D. Y. Zhang, N. Justis and Y. H. Lo, *Appl. Phys. Lett.*, 2004, **84**, 4194–4196.
17 G. R. Xiong, Y. H. Han, C. Sun, L. G. Sun, G. Z. Han and Z. Z. Gu, *Appl. Phys. Lett.*, 2008, 92.
18 L. Pang, U. Levy, K. Campbell, A. Groisman and Y. Fainman, *Opt. Express*, 2005, **13**, 9003–9013.
19 M. A. Unger, H. P. Chou, T. Thorsen, A. Scherer and S. R. Quake, *Science*, 2000, **288**, 113–116.
20 T. Thorsen, S. J. Maerkl and S. R. Quake, *Science*, 2002, **298**, 580–584.
21 K. M. Choi and J. A. Rogers, *J. Am. Chem. Soc.*, 2003, **125**, 4060–4061.
22 H. B. Yu, G. Y. Zhou, F. K. Chau, F. W. Lee, S. H. Wang and H. M. Leung, *Opt. Express*, 2009, **17**, 4782–4790.